THE JOURNAL OF PHYSICAL CHEMISTRY Letters

Letter

Cite This: J. Phys. Chem. Lett. 2018, 9, 5624−5629

pubs.acs.org/JPCL

Stability of Hydrogen Hydrates from Second-Order Møller−Plesset Perturbation Theory

Jan Košata,[‡] Padryk Merkl,[¶] Pattanasak Teeratchanan,[§] and Andreas Hermann*

Centre for Science at Extreme Conditions and SUPA, School of Physics and Astronomy, The University of Edinburgh, Edinburgh EH9 3FD, United Kingdom

Supporting Information

ABSTRACT: The formation of gas hydrates and clathrates critically depends on the interaction between the host water network and the guest gas species. Density functional calculations can struggle to quantitatively capture these dispersion-type interactions. Here, we report wave function-based calculations on hydrogen hydrates that combine periodic Hartree−Fock with a localized treatment of electronic correlation. We show that local second-order Møller−Plesset perturbation theory (LMP2) reproduces the stability of the different filled-ice-like hydrates in excellent agreement with experimental data. In contrast to various dispersion-corrected density functional theory implementations, LMP2 correctly identifies the pressures needed to stabilize the C_0, C_1, and C_2 hydrates and does not find a spurious region of stability for an ice-I_h-based dihydrate. Our results suggest that LMP2 or similar approaches can provide quantitative insights into the mechanisms of formation and eventual decomposition of molecular host−guest compounds.

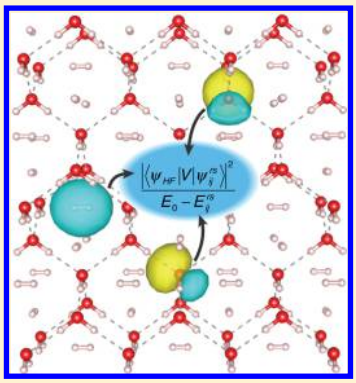

Downloaded via UNIV OF EDINBURGH on September 13, 2018 at 08:08:18 (UTC).
See https://pubs.acs.org/sharingguidelines for options on how to legitimately share published articles.

Gas hydrates, compounds where simple atomic or molecular gases are encapsulated inside a water host network, are materials important for energy and climate science. They are characterized by weak hydrophobic-hydration interactions between the host network and the guest gas species[1] and usually require modest pressures to be stabilized.[2] They are abundant in nature: methane clathrate hydrate covers large sections of the ocean floors[3] and is believed to have been a major component of planetary nebulas that formed the icy bodies of the outer solar system.[4] Gas hydrates also have potential technological applications, in gas transport and storage, and are a known cause of pipe blockage in natural gas extraction.[5,6] In recent years, it has been demonstrated that gas hydrates can be "emptied" (thereby producing new polymorphs of ice[1,7]) and subsequently refilled with different guest species.[8] Accurate computational modeling is indispensable to accompany these efforts of engineering new hydrates.

Hydrogen hydrates have been investigated extensively by experiment and theory because of their large hydrogen weight content, which is ideal for benign hydrogen storage, and their potential occurrence in icy satellites.[7,9−15] Hydrates C_1 and C_2, based on filled ice-II and filled ice-I_c, with H_2:H_2O ratios of 1:6 and 1:1, respectively,[9] have long been known, in addition to a cubic clathrate hydrate, based on the sII structure, at lower pressures.[10] A series of recent experiments found and resolved another hydrate, C_0, based on a new chiral water network, S_χ, also known as ice-XVII.[7,11−14] Density functional theory (DFT) calculations are able to describe this sequence of hydrates and assign C_0 to be a dihydrate, with H_2:H_2O = 1:2,[14−17] but do not agree quantitatively with experiment regarding its region of stability. DFT also consistently predicts an ice-I_h-based dihydrate to supersede C_0 at higher pressure, which has not been seen in experiment.

However, the various interactions at play in gas hydrates are difficult to capture by DFT methods. First and foremost, the weak host−guest interactions, dominantly of dispersion-type, are usually not accessible to semilocal exchange−correlation functionals of the LDA or GGA type. However, dispersion-corrected functionals do not necessarily provide better results; calculations of hydrogen hydrates with the empirical D2 correction scheme or the density-based vdW-DF and vdW-DF2 correlation functionals[18−22] all incorrectly predict that both the C_0 and C_1 hydrates should be stable already at atmospheric pressure.[15,17] Future functional developments might capture the physics of the weak interactions typically present in hydrates better. Post-DFT methods, based on either quantum chemistry or quantum Monte Carlo approaches, have emerged in recent years as promising tools to describe molecular crystals more accurately.[23−27] Second-order Møller−Plesset perturbation theory (MP2) has been applied successfully to individual ice polymorphs, in incremental or fragment schemes,[28,29] a local-MP2 (LMP2) approach,[30] and a fully periodic implementation.[31] MP2 has also been used to simulate bulk liquid water[32] and is generally able to describe hydrogen-bonded systems quite accurately (in particular involving water molecules)[28,33] but also adsorption properties of molecular hydrogen.[34] Diffusion Monte Carlo (DMC) lattice energies have been obtained for various ice phases[35] and for methane clathrate hydrate,[36] with which MP2 results

Received: July 23, 2018
Accepted: September 4, 2018
Published: September 4, 2018

© XXXX American Chemical Society

DOI: 10.1021/acs.jpclett.8b02274
J. Phys. Chem. Lett. 2018, 9, 5624−5629

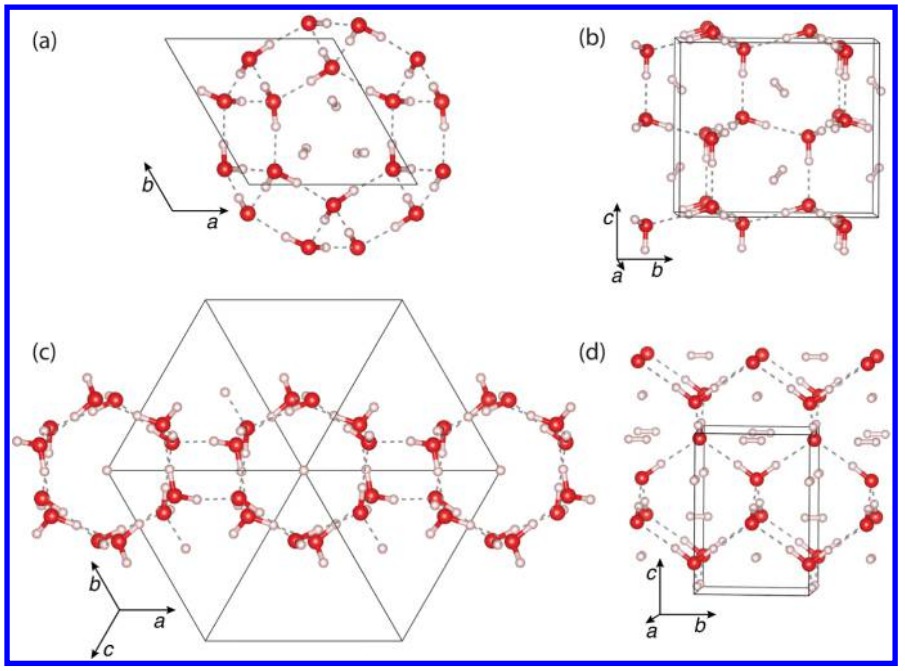

Figure 1. Crystal structures of the hydrogen hydrates considered in this study, all drawn to the same scale. Red and white spheres denote O and H atoms, respectively. Unit cells are indicated by solid black lines, and hydrogen bonds are shown as dashed lines. (a) C_0 hydrate, (b) I_h hydrate, (c) C_1 hydrate, and (d) C_2 hydrate.

compare favorably.[37] LMP2 calculations have been performed on the high-pressure phase behavior of N_2 and CO_2 and show very good agreement with experimental phase diagrams.[38,39]

In this Letter, we report LMP2 and DFT-B3LYP calculations of the binary hydrogen−water system under pressure, where we consider the known hydrates of different stoichiometries and evaluate their stability against each other and decomposition into the constituents. We demonstrate that the LMP2 approach gives very good agreement with experimental results and suggest it should be considered more widely for the description of hydrates and other host−guest compounds.

We consider the hydrogen hydrates shown in Figure 1: the known hydrates C_0 (with a 1:2 H_2:H_2O ratio), C_1 (1:6), and C_2 (1:1), as well as filled ice-I_h (1:2, and using a dipole-free eight-molecule unit cell to model the I_h water network). To establish their stability against decomposition, we consider the ice phases XI (space group $Cmc2_1$), II, and VIII, as well as the chiral water network S_χ of the C_0 hydrate, now known as ice-XVII.[7] Pure hydrogen's free-rotor phase-I is modeled in an eight-molecule cell of $P6_3/m$ symmetry.[40] From the enthalpies of the various hydrates (and the constituents ice and hydrogen) we can construct the binary water−hydrogen phase diagram. We do not consider zero-point energies here, which we expect to effect only small quantitative changes, as seen previously in DFT calculations of hydrogen hydrates.[15] One reason for this is that hydrate formation does not lead to changes in the chemical bonding, and the local environments of the constituents (e.g., water's tetrahedral coordination) are largely unchanged across the different structures. This suggests zero-point energies of hydrates and constituents, dominated by the molecular vibrons, would be very similar at comparable pressures; equilibrium properties could change by a few percent.[41]

We then obtain the stable phases under specific pressure conditions from the convex hull of the relative enthalpies

$$\Delta H_f(x) = \frac{1}{m+n}[H_f(\mathrm{Hy}) - mH_f(H_2O) - nH_f(H_2)] \quad (1)$$

where $x = n/(m+n)$ is the molar hydrogen content of the hydrate $\mathrm{Hy} \equiv (H_2O)_m(H_2)_n$. The compounds on the convex hull of $\Delta H_f(x)$ are stable against all possible decomposition reactions.

In Figure 2 we show the LMP2 cohesive energies for the pure ice phases (see the Supporting Information for pure

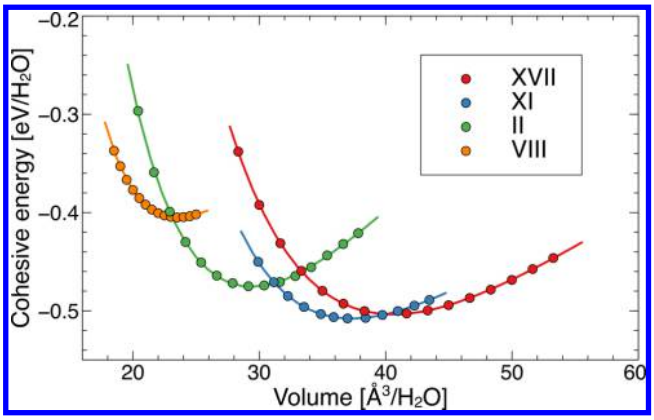

Figure 2. Cohesive energies of various water networks as a function of volume, from counterpoise (CP) corrected LMP2 $E(V)$ data (circles), and fits with the Vinet equation of state (solid lines).

hydrogen results). These demonstrate that LMP2 can capture the correct phase sequence of ice: ice-XI has the lowest cohesive energy overall, with subsequent transitions at high pressures (small volumes) first to ice-II and then to ice-VIII; ice-XVII is metastable, as expected. The equilibrium properties of the different ice phases, obtained from the equation of state (EOS) fits, agree well with experimental data, see Table 1, but have a tendency to underestimate the binding energies. This

DOI: 10.1021/acs.jpclett.8b02274
J. Phys. Chem. Lett. 2018, 9, 5624−5629

Table 1. Ground-State Properties of Water Ice Phases from CP-Corrected LMP2 $E(V)$ Data[a])

ice	E_b [eV]	V_0 [Å^3]	B_0 [GPa]	B_0'
XVII	−0.504	40.58	7.65	4.43
	(−0.623)	(34.85)	(9.16)	(4.41)
		(*35.0*[42])		
XI	−0.508	37.28	8.14	5.20
	(−0.63)	(32.09)	(10.52)	(4.47)
(I_h)	(*−0.61*[43])	(*32.5*[44])	(*9.2*[44])	(*5.5*[44])
II	−0.475	29.36	11.27	4.26
	(−0.549)	(26.50)	(12.23)	(5.22)
	(*−0.61*[43])	(*25.35*[45])	(*14.8*[46])	
VIII	−0.405	23.54	11.49	6.11
	(−0.429)	(21.45)	(15.50)	(6.53)
	(*−0.58*[43])	(*20.6*[47])	(*21.7*[47])	(*4.7*[47])

[a]Equilibrium properties include lattice energies (E_b) and volumes (V_0) (both given per molecule), bulk moduli (B_0), and their pressure derivatives ($B_0' = dB/dP$). Numbers in parentheses are from B3LYP calculations and experiment (italicized: ref 42, T = 25 K; ref 43, 0 K; ref 44, 248 K; ref 45, 110 K; ref 46, 200 K; ref 47, 80 K).

correlates with overestimates of the equilibrium volumes. The corresponding B3LYP results (see the Supporting Information for $E(V)$ plots) deviate less from experiment. With LMP2, we predict the phase transitions from ice-XI to ice-II and from ice-II to ice-VIII to occur at 0.71 and 2.15 GPa, respectively (1.86 and 4.03 GPa with B3LYP). In experiment, these transitions are not observed directly because of the presence of intermediate ice phases not considered here, but one could estimate them to occur roughly around 0.3 and 1.2 GPa, respectively.[48] The LMP2 transition pressures are thus of similar quality as the best results from dispersion-corrected DFT functionals.[49] The parametric formation enthalpies $H_f(p(V)) = E(V) + p(V)V$ of all three ice phases are combined to give the ice formation enthalpy $H_f(H_2O)$ in eq 1.

We then determine the EOS for the different hydrogen hydrates, see Figure 3 and the Supporting Information for full details of the fits. While these can not be compared against one another, because of different compositions, they illustrate the validity of the EOS fits, which form the basis for all enthalpy considerations that follow. The calculated pressure $P = -\partial E/\partial V$ at the smallest volume data point of I_h-hydrate is 3.32 GPa, while those of all other hydrates exceed 9.9 GPa. The smallest

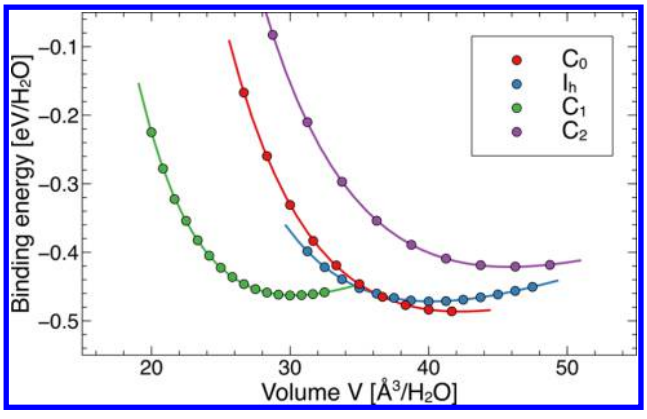

Figure 3. Cohesive energies of various hydrogen hydrates as a function of volume, from CP-corrected LMP2 energies (circles) and fitted to the Vinet EOS (solid lines). Energies are normalized per water molecule.

volume data point of ice-VIII has a pressure of 5.64 GPa, and for hydrogen it is 4.85 GPa. We are therefore confident to discuss reaction enthalpies up to 5 GPa, as they require virtually no EOS-based extrapolation of the LMP2 data, and construct convex hull diagrams for a sequence of pressures up to that point. In the top panel of Figure 4 we show two

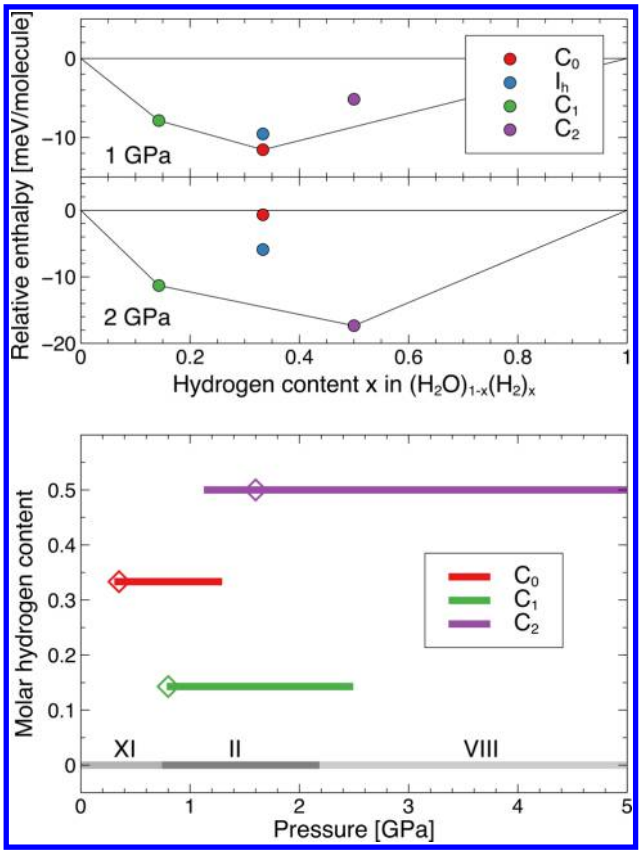

Figure 4. Top panel: two convex hull constructions of hydrates' stabilities at 1 and 2 GPa. Bottom panel: the full phase diagram of hydrogen hydrates, from LMP2 calculations. Regions of stability for the individual hydrates (solid lines) are shown as a function of pressure and hydrogen content. Experimental low-temperature onsets of stability of different hydrates from ref 12 are indicated by diamond symbols. For reference, the calculated phase sequence of water ices is shown as gray lines.

representative convex hulls. At 1 GPa, we find both C_0 and C_1 hydrates to be stable. The I_h-hydrate is less stable than C_0, and C_2 is unstable against formation of C_0 and excess hydrogen. At 2 GPa, C_1 remains stable and C_2 is now also a stable phase, while both C_0 and I_h-hydrate are unstable.

From similar convex hull constructions on much finer pressure grids we then obtain the overall stability ranges of every single hydrate. This data is compiled in the lower panel of Figure 4, which also includes experimental formation pressures of the different hydrates extrapolated to low temperatures.[12] The LMP2 calculations show excellent agreement with the experimental data: they correctly predict the onset of the C_0 and C_1 hydrates at 0.35 and 0.8 GPa, respectively, with a small underestimation of the formation pressure of C_2 (1.16 GPa in calculations vs 1.6 GPa in experiment). Note that we do not consider the clathrate structure sII, because of the high computational demand, which might shift the onset of stability of C_0 to slightly higher

DOI: 10.1021/acs.jpclett.8b02274
J. Phys. Chem. Lett. 2018, 9, 5624−5629

pressures. The full stability ranges of all hydrates are compared with results from B3LYP and other DFT functionals in Table 2. An important result from the LMP2 calculations is that they

Table 2. Stability Ranges of Hydrogen Hydrates from LMP2 and B3LYP Calculations, Compared to Experimental Low-Temperature Estimates and Other DFT Results[a]

	C_0	I_h	C_1	C_2
exptl[12]	0.35−...	−	0.8−...	1.6−...
LMP2	0.34−1.26	−	0.82−2.46	1.16−...
B3LYP	0.77−2.20	2.20−3.36	1.91−...	2.77−...
optB88-vdw[15]	0.00−0.35	0.35−1.5	0.00−3.5	1.5−...
rPW86-vdW2[17]	0.00−0.11	0.11−1.60	0.01−2.62	0.88−...
PBE+D2[17]	0.00−0.24	0.24−1.53	0.81−2.87	1.25−...
PBE[17]	0.86−2.01	2.01−4.00	2.52−...	3.30−...

[a]All pressures are given in GPa.

do not return any region of stability for a I_h-hydrate, which is in agreement with current experimental knowledge, but not with the DFT calculations. The dispersion-corrected functionals included here (vdW-DF, vdW-DF2, and D2) also predict the C_0 hydrate to be stable at atmospheric pressure already; while the functionals that lack explicit inclusion of dispersion corrections (B3LYP and PBE) are qualitatively better in that they stabilize C_0 only at finite pressures.

We have previously shown that the weak interaction of the $H_2O\cdots H_2$ dimer is quite well described with PBE, while dispersion-corrected functionals significantly overbind this interaction.[16] It is possible that this overbinding of the dimer translates into a spurious stabilization of the extended hydrogen hydrates. On the other hand, both B3LYP and PBE predict too large stabilization ranges for all hydrates (compared with LMP2) and delayed onsets of stability for all hydrates (compared with experiment) and feature the I_h-hydrate in an intermediate pressure region. The first two effects could be related to the significant overestimation of the transition pressures in the pure ice phases with these functionals. An ad-hoc rescaling of the PBE and B3LYP stability regions given in Table 2 by a factor of 0.5 results in quite good agreement overall across all hydrogen hydrates. This will not affect the emergence of the I_h-hydrate, which is due to the energy balance between the C_0 and I_h-hydrates, and their high-pressure decomposition into C_1 and C_2. In fact, the LMP2 calculations also predict that I_h-hydrate is more stable than C_0 above 1.3 GPa, but this is just above the pressure where both these hydrates are predicted to decompose into C_1 and C_2. In the Supporting Information, we show the distance of the I_h-hydrate from the convex hull (i.e., its energetic instability) as a function of pressure; in the LMP2 calculations, it comes very close to being, but never is, stable.

In summary, we have presented a comprehensive energetic analysis of hydrogen hydrates using wave function-based local-MP2 calculations. This level of theory should be capable of capturing the weak host−guest interactions that are crucial to the formation of any gas hydrate. Indeed, our results demonstrate that this methodology can be used to understand the complex interplay of different phases under pressure, as it reproduces the formation and eventual decomposition conditions of the different hydrates in very good agreement with experiment. The LMP2 results for the high-pressure evolution of pure water ice are of quality comparable to the best dispersion-corrected DFT functionals, while for the hydrogen hydrates they represent a qualitative improvement, regarding both the onset of the first hydrate phase, C_0, at moderate pressures and the nonappearance of an ice-I_h hydrate. Potential avenues to build upon these results include consideration of higher-order correlation effects, e.g. by incremental corrections;[23] full optimization of geometric degrees of freedom at MP2 level;[28,50] and subsequent consideration of vibrational entropies. We expect that similar wave function-based calculations can capture the essential interactions in other high-pressure systems that are dominated by weak interactions between host matrices and guest species, such as filled zeolites.

COMPUTATIONAL METHODOLOGY

We performed LMP2 calculations using the CRYSTAL14 and CRYSCOR09 software packages.[51,52] Each structure's lattice and atomic positions were optimized at a sequence of unit cell volumes at the B3LYP level of theory.[53] B3LYP geometries were previously found to be very close to MP2 geometries for isolated small molecules (such as water) and for ice.[54−56] We then obtained the Hartree−Fock energies and wave functions for those geometries. Reciprocal space was sampled using regular (8, 8, 8) grids. Subsequent LMP2 calculations involve the construction of Wannier orbitals based on molecular domains (see the Supporting Information for an example), from which the LMP2 amplitudes were determined. Two-electron integrals for pairs of Wannier orbitals separated by less than 6 Å (13 Å) were evaluated using the density fitting (multipole expansion) approaches; longer-range interactions were included in a Lennard-Jones extrapolation. We used triple-ζ basis sets with additional polarization functions (TZP) for both oxygen and hydrogen, as used previously in a study of ice-XI polymorphs.[57] For comparison, the Supporting Information shows results obtained using Pople's 6-311G(d,p) basis set, which was also used for ice-XI previously; we find that this standard basis set performs roughly equal at the B3LYP level but less well at LMP2 level. Basis set superposition errors were corrected with the counterpoise (CP) method, where energies of all molecular entities are recalculated in the presence of "ghost" basis functions in the exact configuration present in the extended solids.[58] Specifically, the CP-corrected energy $E^{CP}_{MP2}(Hy)$ of a hydrate $Hy \equiv (H_2O)_m(H_2)_n$ was determined as

$$E^{CP}_{MP2}(Hy) = E^{0}_{MP2}(Hy) - mE_g(H_2O) - nE_g(H_2) - \sum_{i=1}^{m}\left(E^{gh}_{Hy}(H_2O_i) - E_{Hy}(H_2O_i)\right) - \sum_{j=1}^{n}\left(E^{gh}_{Hy}(H_{2j}) - E_{Hy}(H_{2j})\right) \quad (2)$$

There, E^{0}_{MP2} are the *un*-corrected LMP2 energies; E_g are the MP2-optimized gas phase energies for the H_2O and H_2 molecules (see the Supporting Information for the details of their potential energy surfaces); E_{Hy} are the molecular energies of bare molecules in their crystalline geometry; and E^{gh}_{Hy} are the molecular energies in the presence of "ghost" basis functions. We found that basis functions within a spherical radius of 6 Å around the molecular species give sufficiently converged energies (see the Supporting Information). The resulting $E^{CP}_{MP2}(V)$ data points were fitted to the Vinet equation of

DOI: 10.1021/acs.jpclett.8b02274
J. Phys. Chem. Lett. 2018, 9, 5624−5629

state,[59] which then enabled a parametric determination of the formation enthalpies $H_f(p(V)) = E(V) + p(V)V$.

DFT calculations with dispersion-corrected functionals used the VASP package with "hard" PAW data sets and a plane-wave cutoff energy of 875 eV.[60,61] All geometries were optimized until residual force components were below 2 meV/Å.

■ ASSOCIATED CONTENT

Supporting Information

The Supporting Information is available free of charge on the ACS Publications website at DOI: 10.1021/acs.jpclett.8b02274 Input and output data from the calculations are accessible on the University of Edinburgh's Datashare repository at http://datashare.is.ed.ac.uk/.

Examples of Wannier orbitals, LMP2 energies of H_2 and H_2O molecules, convergence of BSSE-CP correction, EOS of hydrogen phase-I, hydrate data from B3LYP, (in)stability of I_h-hydrate, and 6-311G(d,p) basis set calculations (PDF)

■ AUTHOR INFORMATION

Corresponding Author

*E-mail: a.hermann@ed.ac.uk.

ORCID

Andreas Hermann: 0000-0002-8971-3933

Present Addresses

‡J.K.: Institute for Theoretical Physics, ETH Zürich, 8093 Zürich, Switzerland.

¶P.M.: Department of Microbiology, Tumor and Cell Biology, Karolinska Institutet, 17177 Stockholm, Sweden.

§P.T.: Department of Physics, Faculty of Science, Srinakharinwirot University, Bangkok, Thailand 10110.

Notes

The authors declare no competing financial interest.

■ ACKNOWLEDGMENTS

The authors thank Prof. Beate Paulus and Dr. Casten Müller for fruitful discussions of local correlation methods. Computational resources provided by EPSRC via the UKCP consortium (EP/P022790/1), the UK National Supercomputing Service (project ID d56 "Planetary Interiors"), and the Royal Society (RG-150247) are gratefully acknowledged. P.T. acknowledges support from a Royal Thai Scholarship.

■ REFERENCES

(1) Falenty, A.; Hansen, T. C.; Kuhs, W. F. Formation and properties of ice XVI obtained by emptying a type sII clathrate hydrate. *Nature* **2014**, *516*, 231−233.

(2) Loveday, J. S.; Nelmes, R. J. High-pressure gas hydrates. *Phys. Chem. Chem. Phys.* **2008**, *10*, 937−50.

(3) Hoffmann, R. Old Gas, New Gas. *Am. Sci.* **2006**, *94*, 16−18.

(4) Lunine, J. I.; Stevenson, D. J. Clathrate and ammonia hydrates at high pressure: Application to the origin of methane on Titan. *Icarus* **1987**, *70*, 61−77.

(5) Sloan, E. D., Jr. Fundamental principles and applications of natural gas hydrates. *Nature* **2003**, *426*, 353−363.

(6) Bradshaw, R. W.; Greathouse, J. A.; Cygan, R. T.; Simmons, B. A.; Dedrick, D. E.; Majzoub, E. H. *Desalination Utilizing Clathrate Hydrates (LDRD Final Report)*; 2008; pp 1−80.

(7) Del Rosso, L.; Celli, M.; Ulivi, L. New porous water ice metastable at atmospheric pressure obtained by emptying a hydrogen-filled ice. *Nat. Commun.* **2016**, *7*, 13394.

(8) Kuhs, W. F.; Hansen, T. C.; Falenty, A. Filling Ices with Helium and the Formation of Helium Clathrate Hydrate. *J. Phys. Chem. Lett.* **2018**, *9*, 3194−3198.

(9) Vos, W. L.; Finger, L. W.; Hemley, R. J.; Mao, H.-k. Novel H_2-H_2O clathrates at high pressures. *Phys. Rev. Lett.* **1993**, *71*, 3150−3153.

(10) Mao, W. L.; Mao, H.-k.; Goncharov, A. F.; Struzhkin, V. V.; Guo, Q.; Hu, J.; Shu, J.; Hemley, R. J.; Somayazulu, M.; Zhao, Y. Hydrogen Clusters in Clathrate Hydrate. *Science* **2002**, *297*, 2247−2249.

(11) Efimchenko, V. S.; Kuzovnikov, M. A.; Fedotov, V. K.; Sakharov, M. K.; Simonov, S. V.; Tkacz, M. New phase in the water-hydrogen system. *J. Alloys Compd.* **2011**, *509*, S860−S863.

(12) Strobel, T. A.; Somayazulu, M.; Hemley, R. J. Phase Behavior of $H_2 + H_2O$ at High Pressures and Low Temperatures. *J. Phys. Chem. C* **2011**, *115*, 4898−4903.

(13) Strobel, T. A.; Somayazulu, M.; Sinogeikin, S. V.; Dera, P.; Hemley, R. J. Hydrogen-Stuffed, Quartz-like Water Ice. *J. Am. Chem. Soc.* **2016**, *138*, 13786−13789.

(14) Amos, D. M.; Donnelly, M.-E.; Teeratchanan, P.; Bull, C. L.; Falenty, A.; Kuhs, W. F.; Hermann, A.; Loveday, J. S. A Chiral Gas-Hydrate Structure Common to the Carbon Dioxide-Water and Hydrogen-Water Systems. *J. Phys. Chem. Lett.* **2017**, *8*, 4295−4299.

(15) Qian, G.-R.; Lyakhov, A. O.; Zhu, Q.; Oganov, A. R.; Dong, X. Novel Hydrogen Hydrate Structures under Pressure. *Sci. Rep.* **2015**, *4*, 5606.

(16) Teeratchanan, P.; Hermann, A. Computational phase diagrams of noble gas hydrates under pressure. *J. Chem. Phys.* **2015**, *143*, 154507.

(17) Teeratchanan, P. *First-principles studies of gas hydrates and clathrates under pressure*. Ph.D. Thesis, The University of Edinburgh, 2017.

(18) Grimme, S. Semiempirical GGA-Type Density Functional Constructed with a Long-Range Dispersion Correction. *J. Comput. Chem.* **2006**, *27*, 1787−99.

(19) Dion, M.; Rydberg, H.; Schröder, E.; Langreth, D. C.; Lundqvist, B. I. Van der Waals Density Functional for General Geometries. *Phys. Rev. Lett.* **2004**, *92*, 246401.

(20) Román-Pérez, G.; Soler, J. M. Efficient Implementation of a van der Waals Density Functional: Application to Double-Wall Carbon Nanotubes. *Phys. Rev. Lett.* **2009**, *103*, 096102.

(21) Klimeš, J.; Bowler, D. R.; Michaelides, A. Chemical accuracy for the van der Waals density functional. *J. Phys.: Condens. Matter* **2010**, *22*, 022201.

(22) Lee, K.; Murray, É. D.; Kong, L.; Lundqvist, B. I.; Langreth, D. C. Higher-accuracy van der Waals density functional. *Phys. Rev. B: Condens. Matter Mater. Phys.* **2010**, *82*, 081101.

(23) Müller, C.; Usvyat, D. Incrementally Corrected Periodic Local MP2 Calculations: I. The Cohesive Energy of Molecular Crystals. *J. Chem. Theory Comput.* **2013**, *9*, 5590−5598.

(24) Yang, J.; Hu, W.; Usvyat, D.; Matthews, D.; Schütz, M.; Chan, G. K.-L. Ab initio determination of the crystalline benzene lattice energy to sub-kilojoule/mol accuracy. *Science* **2014**, *345*, 640−643.

(25) Steenbergen, K. G.; Gaston, N.; Müller, C.; Paulus, B. Method of increments for the halogen molecular crystals: Cl, Br, and I. *J. Chem. Phys.* **2014**, *141*, 124707.

(26) Beran, G. J. O. Modeling Polymorphic Molecular Crystals with Electronic Structure Theory. *Chem. Rev.* **2016**, *116*, 5567−5613.

(27) Červinka, C.; Beran, G. J. O. Ab initio prediction of the polymorph phase diagram for crystalline methanol. *Chem. Sci.* **2018**, *9*, 4622−4629.

(28) Hermann, A.; Schwerdtfeger, P. Ground-State Properties of Crystalline Ice from Periodic Hartree-Fock Calculations and a Coupled-Cluster-Based Many-Body Decomposition of the Correlation Energy. *Phys. Rev. Lett.* **2008**, *101*, 183005.

(29) Nanda, K. D.; Beran, G. J. O. What Governs the Proton Ordering in Ice XV? *J. Phys. Chem. Lett.* **2013**, *4*, 3165−3169.

(30) Pisani, C.; Maschio, L.; Casassa, S.; Halo, M.; Erba, A. A local-MP2 approach to the ab initio study of electron correlation in crystals

DOI: 10.1021/acs.jpclett.8b02274
J. Phys. Chem. Lett. 2018, 9, 5624−5629

and to the simulation of vibrational spectra: the case of Ice XI. *Theor. Chem. Acc.* **2009**, *123*, 327−335.
(31) Del Ben, M.; Vandevondele, J.; Slater, B. Periodic MP2, RPA, and Boundary Condition Assessment of Hydrogen Ordering in Ice XV. *J. Phys. Chem. Lett.* **2014**, *5*, 4122−4128.
(32) Del Ben, M.; Schönherr, M.; Hutter, J.; VandeVondele, J. Bulk Liquid Water at Ambient Temperature and Pressure from MP2 Theory. *J. Phys. Chem. Lett.* **2013**, *4*, 3753−3759.
(33) Tsatsoulis, T.; Hummel, F.; Usvyat, D.; Schütz, M.; Booth, G. H.; Binnie, S. S.; Gillan, M. J.; Alfè, D.; Michaelides, A.; Grüneis, A. A comparison between quantum chemistry and quantum Monte Carlo techniques for the adsorption of water on the (001) LiH surface. *J. Chem. Phys.* **2017**, *146*, 204108.
(34) Usvyat, D. High precision quantum-chemical treatment of adsorption: Benchmarking physisorption of molecular hydrogen on graphane. *J. Chem. Phys.* **2015**, *143*, 104704.
(35) Santra, B.; Klimeš, J.; Alfè, D.; Tkatchenko, A.; Slater, B.; Michaelides, A.; Car, R.; Scheffler, M. Hydrogen Bonds and van der Waals Forces in Ice at Ambient and High Pressures. *Phys. Rev. Lett.* **2011**, *107*, 185701.
(36) Cox, S. J.; Towler, M. D.; Alfè, D.; Michaelides, A. Benchmarking the performance of density functional theory and point charge force fields in their description of sI methane hydrate against diffusion Monte Carlo. *J. Chem. Phys.* **2014**, *140*, 174703.
(37) Gillan, M. J.; Alfè, D.; Manby, F. R. Energy benchmarks for methane-water systems from quantum Monte Carlo and second-order Møller-Plesset calculations. *J. Chem. Phys.* **2015**, *143*, 102812.
(38) Erba, A.; Maschio, L.; Salustro, S.; Casassa, S. A post-Hartree-Fock study of pressure-induced phase transitions in solid nitrogen: The case of the α, γ, and ϵ low-pressure phases. *J. Chem. Phys.* **2011**, *134*, 074502.
(39) Li, J.; Sode, O.; Voth, G. A.; Hirata, S. A solid-solid phase transition in carbon dioxide at high pressures and intermediate temperatures. *Nat. Commun.* **2013**, *4*, 2647.
(40) Pickard, C. J.; Needs, R. J. Structure of Phase III of Solid Hydrogen. *Nat. Phys.* **2007**, *3*, 473.
(41) Heit, Y. N.; Beran, G. J. O. How important is thermal expansion for predicting molecular crystal structures and thermochemistry at finite temperatures? *Acta Crystallogr., Sect. B: Struct. Sci., Cryst. Eng. Mater.* **2016**, *72*, 514−529.
(42) del Rosso, L.; Grazzi, F.; Celli, M.; Colognesi, D.; Garcia-Sakai, V.; Ulivi, L. Refined Structure of Metastable Ice XVII from Neutron Diffraction Measurements. *J. Phys. Chem. C* **2016**, *120*, 26955−26959.
(43) Whalley, E. Energies of the phases of ice at zero temperature and pressure. *J. Chem. Phys.* **1984**, *81*, 4087−4092.
(44) Shaw, G. H. Elastic properties and equation of state of high pressure ice. *J. Chem. Phys.* **1986**, *84*, 5862−5868.
(45) Kamb, B.; Hamilton, W. C.; LaPlaca, S. J.; Prakash, A. Ordered Proton Configuration in Ice II, from Single-Crystal Neutron Diffraction. *J. Chem. Phys.* **1971**, *55*, 1934−1945.
(46) Lobban, C.; Finney, J. L.; Kuhs, W. F. The p-T dependency of the ice II crystal structure and the effect of helium inclusion. *J. Chem. Phys.* **2002**, *117*, 3928−3934.
(47) Yoshimura, Y.; Stewart, S. T.; Somayazulu, M.; Mao, H.-k.; Hemley, R. J. High-pressure x-ray diffraction and Raman spectroscopy of ice VIII. *J. Chem. Phys.* **2006**, *124*, 024502.
(48) Salzmann, C. G.; Radaelli, P. G.; Slater, B.; Finney, J. L. The polymorphism of ice: five unresolved questions. *Phys. Chem. Chem. Phys.* **2011**, *13*, 18468−18480.
(49) Santra, B.; Klimeš, J.; Tkatchenko, A.; Alfè, D.; Slater, B.; Michaelides, A.; Car, R.; Scheffler, M. On the accuracy of van der Waals inclusive density-functional theory exchange-correlation functionals for ice at ambient and high pressures. *J. Chem. Phys.* **2013**, *139*, 154702.
(50) Del Ben, M.; Hutter, J.; Vandevondele, J. Forces and stress in second order Møller-Plesset perturbation theory for condensed phase systems within the resolution-of-identity Gaussian and plane waves approach. *J. Chem. Phys.* **2015**, *143*, 102803.
(51) Dovesi, R.; Orlando, R.; Erba, A.; Zicovich-Wilson, C. M.; Civalleri, B.; Casassa, S.; Maschio, L.; Ferrabone, M.; De La Pierre, M.; D'Arco, P.; et al. CRYSTAL14: A Program for the Ab Initio Investigation of Crystalline Solids. *Int. J. Quantum Chem.* **2014**, *114*, 1287−1317.
(52) Pisani, C.; Schütz, M.; Casassa, S.; Usvyat, D.; Maschio, L.; Lorenz, M.; Erba, A. Cryscor: a program for the post-Hartree-Fock treatment of periodic systems. *Phys. Chem. Chem. Phys.* **2012**, *14*, 7615−7628.
(53) Becke, A. D. Density-functional thermochemistry. III. The role of exact exchange. *J. Chem. Phys.* **1993**, *98*, 5648−5652.
(54) Finley, J. W.; Stephens, P. J. Density functional theory calculations of molecular structures and harmonic vibrational frequencies using hybrid density functionals. *J. Mol. Struct.: THEOCHEM* **1995**, *357*, 225−235.
(55) Zygmunt, S. A.; Mueller, R. M.; Curtiss, L. A.; Iton, L. E. An assessment of density functional methods for studying molecular adsorption in cluster models of zeolites. *J. Mol. Struct.: THEOCHEM* **1998**, *430*, 9−16.
(56) Erba, A.; Casassa, S.; Dovesi, R.; Maschio, L.; Pisani, C. Periodic density functional theory and local-MP2 study of the librational modes of Ice XI. *J. Chem. Phys.* **2009**, *130*, 074505.
(57) Erba, A.; Casassa, S.; Maschio, L.; Pisani, C. DFT and Local-MP2 Periodic Study of the Structure and Stability of Two Proton-Ordered Polymorphs of Ice. *J. Phys. Chem. B* **2009**, *113*, 2347−2354.
(58) Boys, S. F.; Bernardi, F. The calculation of small molecular interactions by the differences of separate total energies. Some procedures with reduced errors. *Mol. Phys.* **1970**, *19*, 553.
(59) Vinet, P.; Ferrante, J.; Smith, J. R.; Rose, J. H. A universal equation of state for solids. *J. Phys. C: Solid State Phys.* **1986**, *19*, L467−L473.
(60) Kresse, G.; Furthmüller, J. Efficient Iterative Schemes for Ab initio Total-energy Calculations Using a Plane-wave Basis Set. *Phys. Rev. B: Condens. Matter Mater. Phys.* **1996**, *54*, 11169−11186.
(61) Kresse, G.; Joubert, D. From ultrasoft pseudopotentials to the projector augmented-wave method. *Phys. Rev. B: Condens. Matter Mater. Phys.* **1999**, *59*, 1758−1775.

DOI: 10.1021/acs.jpclett.8b02274
J. Phys. Chem. Lett. 2018, 9, 5624−5629